

Appendix O

Noise Below Water from Sonic Booms

1.0 Background

Noise transmission below water is described differently than noise transmission above water. The noise measurement unit used to describe the level of noise transmitted through air is the decibel (dB), commonly based on a reference overpressure of 0.0002 dyne/cm², written specifically as “dB (re 0.0002 Bar).” The same logarithmic unit (dB) is commonly used in underwater acoustics, but with a different reference pressure. The typical reference pressure used in underwater acoustics is one micro-Pascal (1 μPa), written as “dB (re 1 μPa),” where μPa means 10⁻⁶ Pascal. To convert “dB re .0002 Bar” to “dB re 1 μPa,” add 26 dB to the former (i.e., dB [re 1 μPa] = dB [re 0.0002 Bar] + 26) (Pierce, A.D., 1994; Richardson, et al., 1995).

In analogy with classical optics, acoustic-pressure signals can penetrate rather deeply into water, as long as the incident ray angle θ_i measured from the vertical plane does not exceed the critical value $\theta_c = \sin^{-1}(a_A/a_W)$, where (a_A/a_W) is the air-to-water sound-speed ratio. The reciprocal of this ratio is 4.53 (under standard conditions). Therefore, for the incident ray angle $\theta_i < \theta_c = \sin^{-1}(1/4.53) = 12.75^\circ$, penetration of acoustic disturbances deeply into the water is possible. This figure corresponds to the condition that the wave fields move horizontally at supersonic speed both above and below the air-water interface, and that the horizontal Mach number of the vehicle (in steady motion) must be greater than a_W/a_A or 4.53. For $\theta_i > \theta_c = 12.75^\circ$ (corresponding to a horizontal Mach number less than 4.53, commonly found with supersonic aircraft and space launches during the ascending phase), the ray theory as an approximation underlying the sonic boom analysis would predict a “total reflection,” allowing no acoustic energy to be transmitted from air into water. The prediction method based on the ray approximation does not apply underwater for $\theta_i > 12.75^\circ$, so must be replaced by a fuller analysis.

The overpressure level, signature length, and penetration depth underwater depend significantly on the launch vehicle thrust and weight, which determine the sonic boom disturbances from the rocket plume. Therefore, the underwater overpressure levels from the Atlas V system with Solid Rocket Motors (SRMs) and Delta IV system with larger SRMs would be greater than those reported in a study of Minuteman-type launches for the Air Force Atmospheric Interceptor Technology (AIT) program at Kodiak, Alaska (SMC, 1997), and less than those produced by the Titan or Saturn rockets (Cheng and Lee, 1998).

2.0 Underwater Noise Models

Two types of analysis methods for underwater sonic boom noise are available. One is based on the Sawyer method (1968 model), which accounts for the penetration of sonic boom disturbances under a flat ocean. The other model is based on the surface wave influence on

the sonic boom penetration into the deep ocean (Cheng and Lee, 1998). The flat-ocean model is useful in providing the underwater overpressure field not far from the sea surface where potential sonic boom effects on marine mammals pertaining to “Harassment A,” such as the hearing-threshold shift (Bowles and Stewart 1980), may be found. Cheng and Lee’s (1998) model accounting for the surface wave influence furnishes a method for assessing the audibility of the sonic boom noise in deep water, because the interaction effect of sonic boom and a surface wave train has been shown to overwhelm the flat-ocean wavefield at large depth, in frequency range of 5 to 50 Hz, where the overpressure level is low, but still is noticeable above the ambient noise level of 60 to 80 dB (re 1 μ Pa) (Urick, 1983).

Four booms from each launch were selected for the underwater analyses. Using names of the AF trajectory file, the four launches are designated by Eastern Range low earth orbit (ERLEO), Eastern Range geosynchronous transfer orbit (ERGTO), Western Range low earth orbit (WRLEO), and Western Range geosynchronous transfer orbit (WRORB). The four booms for each launch are distinguished as follows: FOC (focus boom on centerline), focus boom at the carpet edge (EDG), centerline carpet boom (CPT) and carpet boom at a position of 1/2 CPT overpressure level (CP2).

Common and similar features of the sea-level waveforms for the booms include: FOC, EDG, CPT, and CP2. Such common features facilitate study and inferences regarding wavefield properties underwater and reduce analysis effort for both flat- and wavy-surface models. Study and assessment based on the wavefield similarities afforded by theories of Sawyer (1968) and Cheng and Lee (1998) must consider not only differences in the overpressure level and overall signature length scale of the input sea-level waveforms, but also the Mach number of the horizontal velocity component of the wavefield. The importance of the horizontal Mach number has been made apparent by examples in Sparrow’s (1995) study. Simulation studies of the sonic-boom and surface-wave interaction show that one must also consider the wave length of the surface-wave train. The latter depends on the sea state (Cheng and Lee 1998). In the discussion described below, Cheng and Lee’s theory is used to assess the surface waviness influence, based on parameters determined from the sea-level overpressure data.

The distinct features shared by the sea-level waveforms of the FOC and EDG are not only the sharp peaks (“rabbit ears”) next to the front and tail shocks, but also the notably low overpressure level elsewhere in the waveform. The latter resembles an asymmetrical N-wave with a tail shock that is 10 to 20 percent weaker than that in the front. While the sea-level CPT of the same launch has a similar asymmetrical N-waveform, it is considerably stronger, which explains why the noise from CPT can dominate an underwater noise field even at a depth that would be small compared to the signature length, because the peaky features of FOC and EDG attenuate rapidly with distance, as have been found for all the launches in the current study. The depth where FOC and EDG effects falls off underwater and the CPT effects takes over seldom exceeds 50 feet for the Delta IV system and 60 feet for the Atlas V system. Above these levels, however, the overpressure levels under a FOC/EDG rise rapidly to match the very high focus boom level (see below). In this 50- to 60-foot upper layer of the ocean, the potential “Harassment A” on marine mammals can be an issue. Overpressure contours in the vertical plane and other wavefield details have been computed for all given sea-level waveforms, and are discussed below.

Under a wavy ocean in a fully developed sea state (Bascom, 1964; Stewart, 1969), the example in Cheng and Lee (1998) has indicated that an incident N-wave from a supersonic aircraft that generates 2 psf peak overpressure at sea level may cause a 100 to 120 dB (re 1 μ Pa) maximum overpressure at a depth of one-half kilometer in the 20 to 25 hertz (Hz) frequency range. These overpressure and frequency ranges are comparable to the dominant part of the vocalization records of blue whale and fin whale calls (Richardson, et al., 1995). The overpressure level mentioned is noticeably higher than the 80 dB (re 1 μ Pa) of the ambient noise of the deep sea in the 20 to 25 Hz range (Urlick, 1983), and should be audible. The surface horizontal Mach numbers of all of the booms considered are much closer to unity (1.08 to 1.12) than the example in Cheng and Lee (1.8). One may expect, according to the theory, that the noise penetration power augmented by surface-wave influence can be several times stronger than was reported by Cheng and Lee (1998). On the other hand, the ratio of surface-wave length to the signature length is smaller for the present problem than for the aircraft example from Cheng and Lee. A close examination of deep-water analysis in Cheng and Lee's solution for the Mach number and surface-wave number yields neither exceedingly high nor low overpressure magnitude. Therefore, the audibility issue remains the same as for the aircraft example indicated above. In summary, the assumption of a flat wave state in the model used in this analysis is expected to yield a rough approximation of actual effects. A definitive study for the waviness and related sea-state issues must await a more concrete analysis.

3.0 Underwater Noise Analysis Results

3.1 Atlas V System with SRMs

The sea-level waveforms from the Atlas V system launches are quite close to one another in each of the four types: the FOC, EDG, CPT, and CP2, with exceptions noted below.

Cape Canaveral Air Force Station

Sonic booms occurring at Cape Canaveral Air Force Station (CCAFS) during several launches from the east range have been considered. Figures O-1 to O-4¹ show the sea-level overpressure waveforms of the Atlas V system LEO launch, marked with the local horizontal Mach numbers, for the four FOC, EDG, CPT and CP2 type booms, respectively. The maximum overpressure at the spiky peak is 7.3 pounds per square foot (psf) in FOC and 3 psf in EDG, while the maximum overpressure is 2.8 psf in CPT and 1.9 psf in EDG. The FOC and EDG waveforms appear to be the results of adding the two spikes (rabbit ears) to a slightly modified N-wave. The signature length of these waveform varies slightly within 600 to 650 feet, except for the longer length, 1,030 feet, in the CP2. The sea-level waveforms for the Atlas V system LEO launch are very close to those shown for Atlas V system GTO.

Among the underwater wavefield data generated by the flat-ocean model for the four types of sea-level waveforms, the plots of the overpressure as a function of depth, z (in feet), are presented and compared in Figure O-5 for the Atlas V system GTO launch from the east range. A significant feature in this comparison, which is shared by all Atlas V system and

¹ All figures follow the text of this appendix.

Delta IV launches under study, is that high overpressures comparable to that on the sea surface are found mainly within the first 60 feet underwater. The plot shows that the magnitudes attenuate rapidly with increasing depth, reducing to 0.3 psf or less at the 400-foot depth. Similar results for an Atlas V system LEO launch with azimuth angle 43° are given in Figure O-6.

Vandenberg AFB

The launches from the west range yield sea-level sonic boom waveforms very close to those from the east range in their respective waveform types, as shown in Figures O-1 to O-4 for Atlas V system LEO. The plots of maximum overpressure versus depth z for the three west-range launches, Atlas V system GTO (94°), Atlas V system LEO (43°) and Atlas V system (158°), are shown in Figures O-5, O-6, and O-7. These figures reveal little variation from launch to launch, and are similar to those of the east-range launches.

3.2 Delta IV System with Larger SRMs

The sea-level waveforms from the Delta IV system launches are almost identical to one another in each of the four types (FOC, EDG, CPT, and CP2), except for those from the ERLEO launch, which yields lower maximum overpressure, but is similar otherwise.

Cape Canaveral Air Force Station

Launches considered from CCAFS are ERGTO and ERLEO launched from the east range. Figures O-8 to O-11 show the sea-level overpressure waveforms, marked also with the local horizontal Mach numbers for FOC, EDG, CPT, and CP2 of the ERGTO, respectively. The maximum overpressure at the spiky peaks is seen to be 7.4 psf in the FOC and about 6 psf in the EDG, while the maximum overpressure is close to 4 psf in the CPT and to a lower 2 psf in the CP2. Notice that the sea-level overpressure immediately after (downstream of) the peak is not far from 2 psf in both FOC and EDG booms, which is certainly lower than the 4 psf maximum of the CPT. The sea-level signature lengths vary only slightly between 485 and 500 feet among various waveform types, with the exception of WRORB which has a shorter length (460 feet) along with a lower maximum overpressure (6 psf). These differences and similarities among the four waveform types that affect/determine the underwater impact are common to most launch results.

From the underwater wavefield computed according to the flat-ocean model, the maximum overpressure underwater is plotted as a function of depth, z (in feet), for each of the sea-level waveforms, as shown in Figure O-12. As noted earlier, the high overpressure level associated with spike-like features in the FOC and EDG attenuates rapidly underwater, but remains significant at a depth of 50 feet. At this depth and below, where the maximum overpressure level is 2 psf, the CPT is seen to dominate. The plot shows that the overpressure level from the CPT can be as high as 1/3 psf at 400 feet below sea level.

Figures O-13 and O-14 show examples of the overpressure contour in the vertical plane for the FOC and CPT sea-level waveforms of the ERGTO launch. The asymmetry in the contour plots in both figures reflects the asymmetry originated from the modified N-waves FOC and CPT sea-level waveforms noted earlier. Comparing the contour plots of the figures reveals clearly the pervasive nature of the CPT boom in the deeper part of the water; it indicates that a 0.10 psf overpressure from the CPT boom can be found at 1,000 feet below

sea level, even in the absence of surface-wave influence. This result is typical of all CPTs of the launch series considered (except for the ERLEO launch, which can reach only 800 feet below sea level).

Figure O-15 compares underwater maximum overpressure for FOC, EDG, CPT, and CP2 sonic boom types generated by the ERLEO launch at various depths down to 400 feet. Most features and remarks noted earlier for Figure O-12 for the ERGTO launch apply equally here, except for the noticeably reduced overpressure levels, which are more than 40 percent lower than in the other cases.

Vandenberg AFB

The maximum overpressure at various depths for FOC, EDG, CPT, and CP2 are shown in Figure O-16 for WRLEO launch. Here, the features and remarks noted earlier on Figure O-12 for the ERGTO launch also apply, except that the maximum overpressure near sea level is slightly higher for the EDG and slightly lower for the CPT. The corresponding plots for the WRORB launch are presented in Figure O-17, which is comparable to results from the ERGTO launch shown in Figure O-12.

Cited References

- Au, W.W.L., P. E. Nachtigal, and K. L. Powlowski. "Acoustic Effects of the ATOC Signal (75 Hz, 195 dB) on Dolphins and Whales." *J. Acoust. Soc. Am.* Vol. 101, No. 5, Pt. 1. 1997.
- Bascom, W. *Waves and Beaches*. Doubleday, Pp. 9-11, 42-59. 1964.
- Bowles, A. E. and B. Stewart. "Disturbances to the Pinnipeds and Birds of San Miquel Island, 1979-1980." *Potential Effects of Space Shuttle Sonic Booms on Biota and Geology of the California Channel Islands: Research Reports*. Tech. Report 81-1, Cent. Mar. Stud. San Diego State Univ. and Hubbs/Sea World Res. Inst. Dan Diego, CA. Pp. 99-137. 1980.
- Bowles, A. E., M. Smultea, B. Wursig, D. P. DeMaster, and D. Palka. "Relative Abundance and Behavior of Marine Mammals Exposed to Transmission from the Heard Island Feasibility Test." *J. Acoust. Soc. Am.* Vol. 96, No. 4, Pp. 2469-2484. 1994.
- Cheng, H. K. and C. J. Lee. "A Theory of Sonic Boom Noise Penetration Under a Wavy Ocean." AIAA Paper 98-2958. 1998.
- Costa, D. P., D. E. Crocker, D. Croll, D. Goley, D. Houser, B. J. LeBouef, D. Waples, and P. Webb. "Effects of California ATOC Experiment on Marine Mammals." *J. Acoust. Soc. Am.* Vol. 100, P. 2581. 1996.
- Frankle, A. S. and C. W. Clark. "Results of Low-Frequency Playback of M-Sequence Noise to Humpback Whales." *Megatera Novaeangliae, In Hawaii, Can. J. Zool.* Vol. 76, Pp. 521-535. 1998.
- Medwin, H., R. A. Helbig, and J. D. Hagy, Jr. "Spectral Characteristics of Sound Transmission through the Rough Sea Surface." *J. Acoust. Soc. America.* Vol. 54, No. 1, Pp. 99-109. 1973.
- Munk, W., P. Worchester, and C. Wunsch. *Ocean Acoustic Tomography*. Cambridge Univ. Press. 1995.

Potter, J. R. "ATOC: Sound Policy or Enviro-Vandalism? Aspect of a Modern Media-Fueled Policy Issue." *J. Environment and Development*. Vol. 3, No. 2, Pp. 47-62. 1994.

Pierce, A. D. *Acoustics*. *Acoustic Soc. Am.* Pp. 75-82. 1994.

Richardson, W. J., et al. *Marine Mammals and Noise*. Acad. Press. Pp. 15-86, 425-452. 1995.

Sawyers, K. H. "Underwater Sound Pressure from Sonic Booms." *J. Acoust. Soc. Am.* Vol. 44, No. 2, Pp. 523-524. 1968.

Sparrow, V. W. "The Effect of Supersonic Aircraft Speed on the Penetration of Sonic Boom Noise into the Ocean." *J. Acoust. Soc. Am.* Vol. 97, No. 1, P. 159-162. 1995.

Stewart, R. H. "The Atmosphere and the Ocean." *The Ocean Scientific American Book*. W. H. Freeman & Co. P. 28-38. 1969.

Urick, R. J. *Principles of Underwater Sound*. 3rd ed. McGraw Hill. 1983.

USAF Material Command. Environment Impact Analysis Process: Environment Assessment for USAF Atmospheric Interceptor Technology Program, Appendix C. Launch Noise and Sonic Boom. 1997.

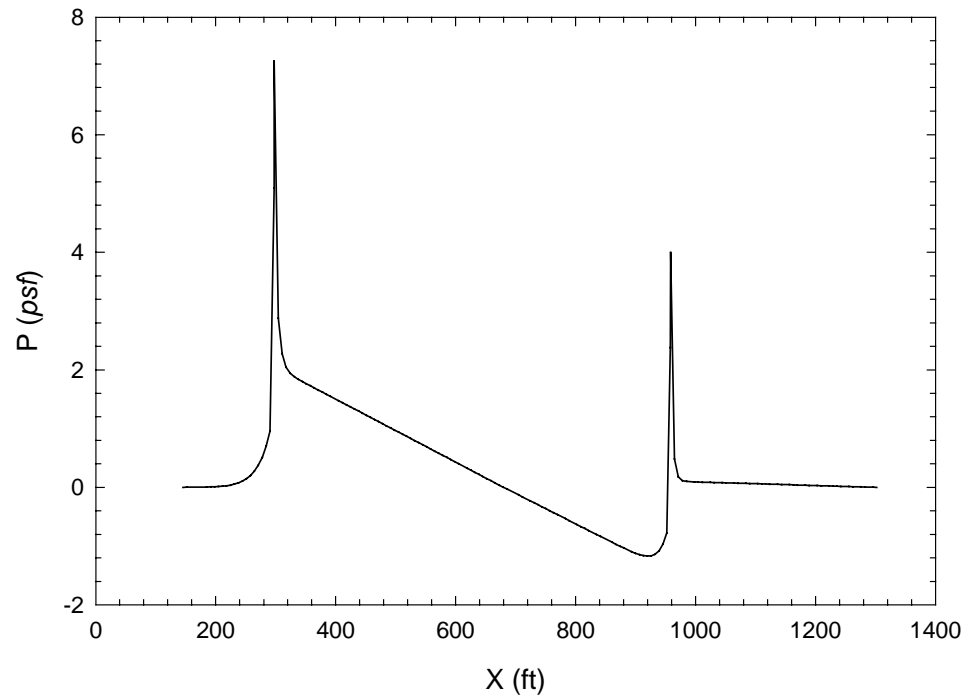


Figure O-1

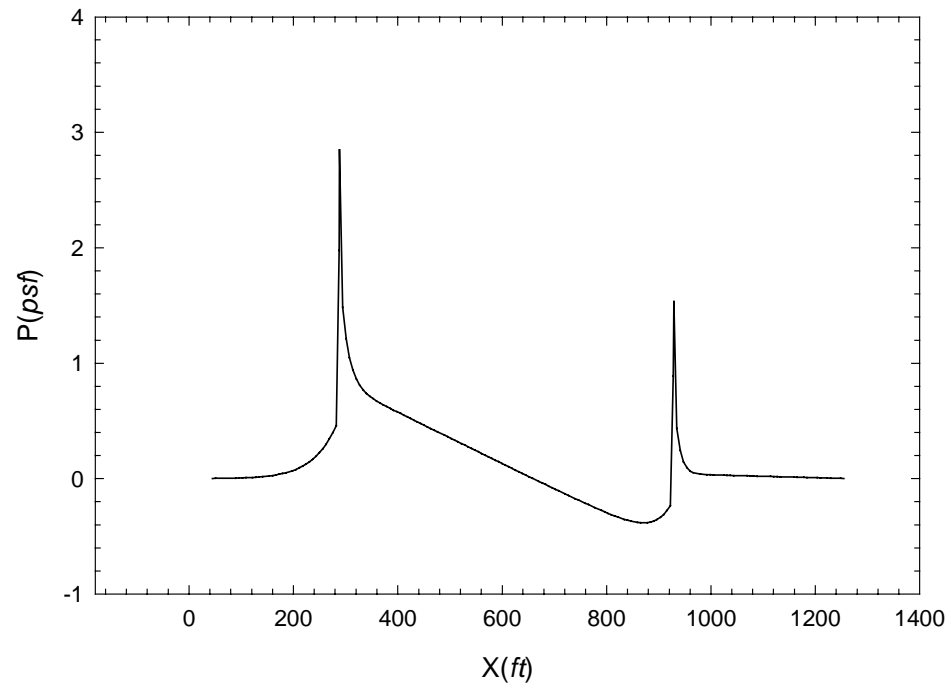


Figure O-2

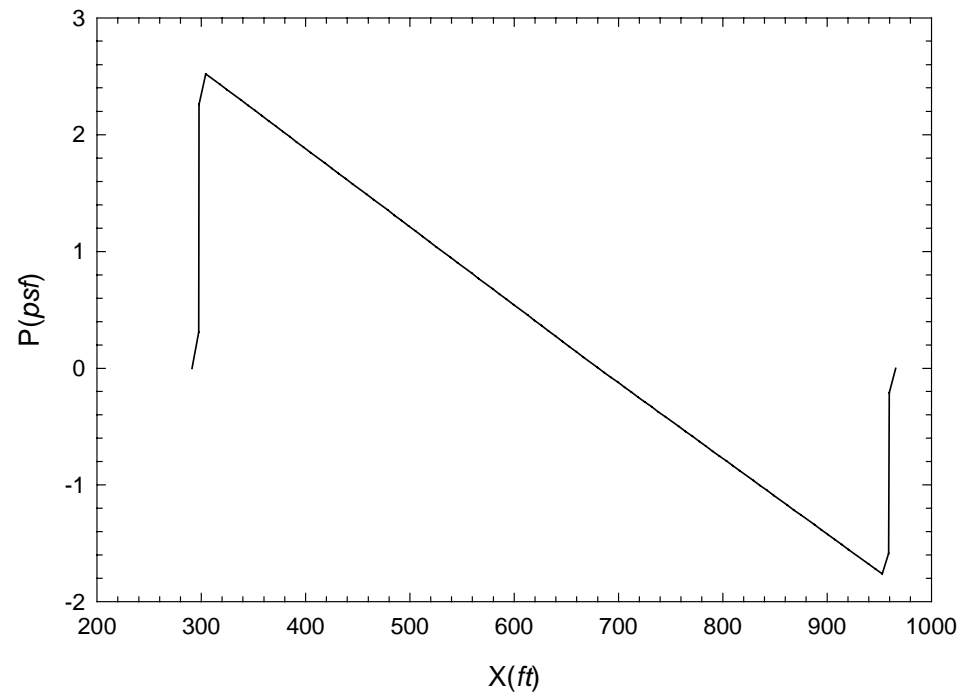


Figure O-3

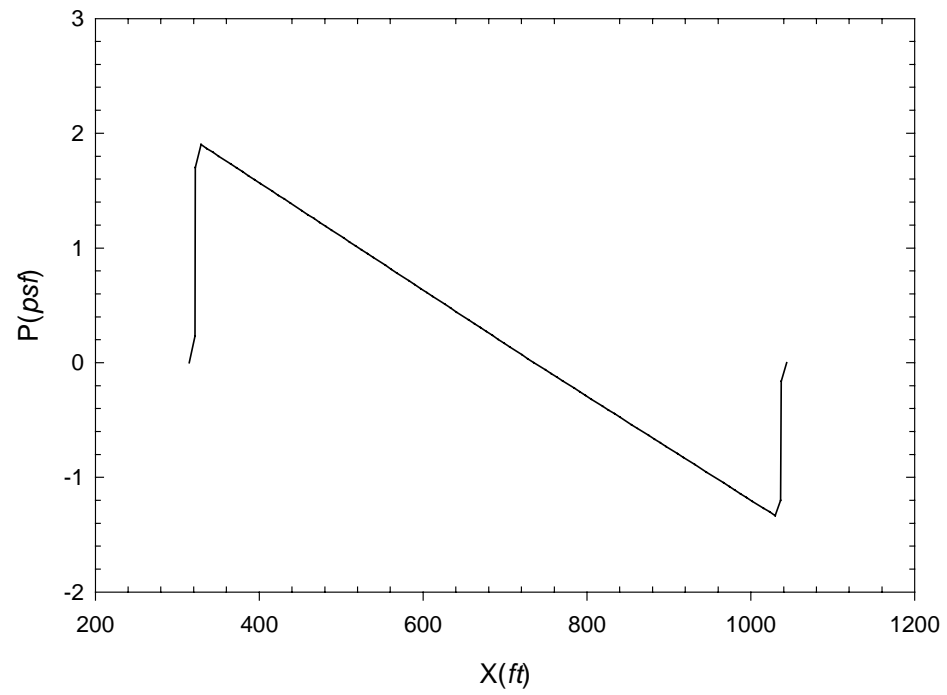


Figure O-4

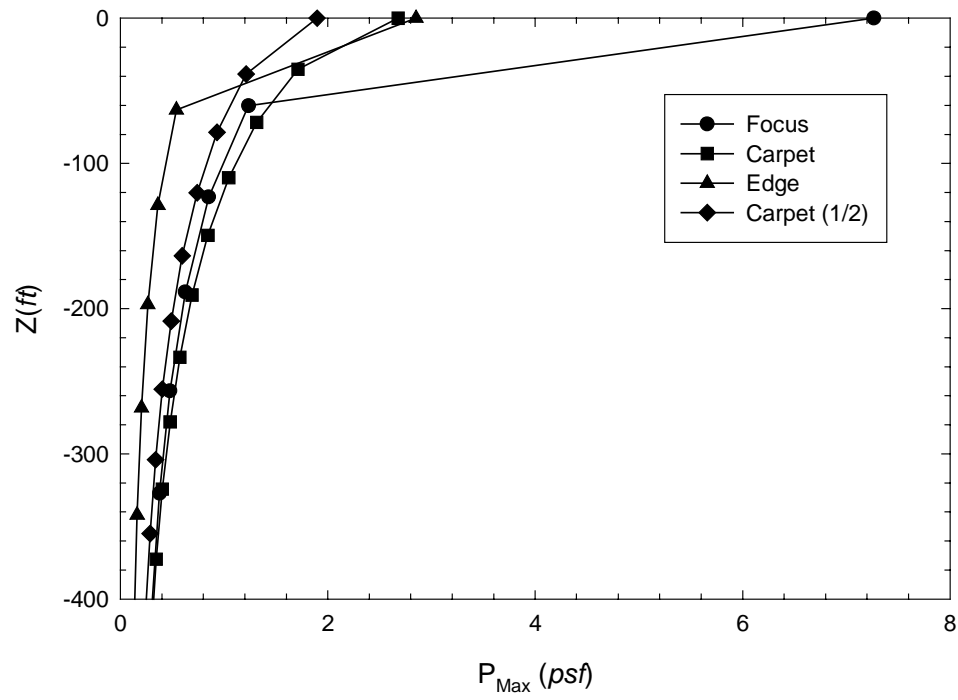


Figure O-5

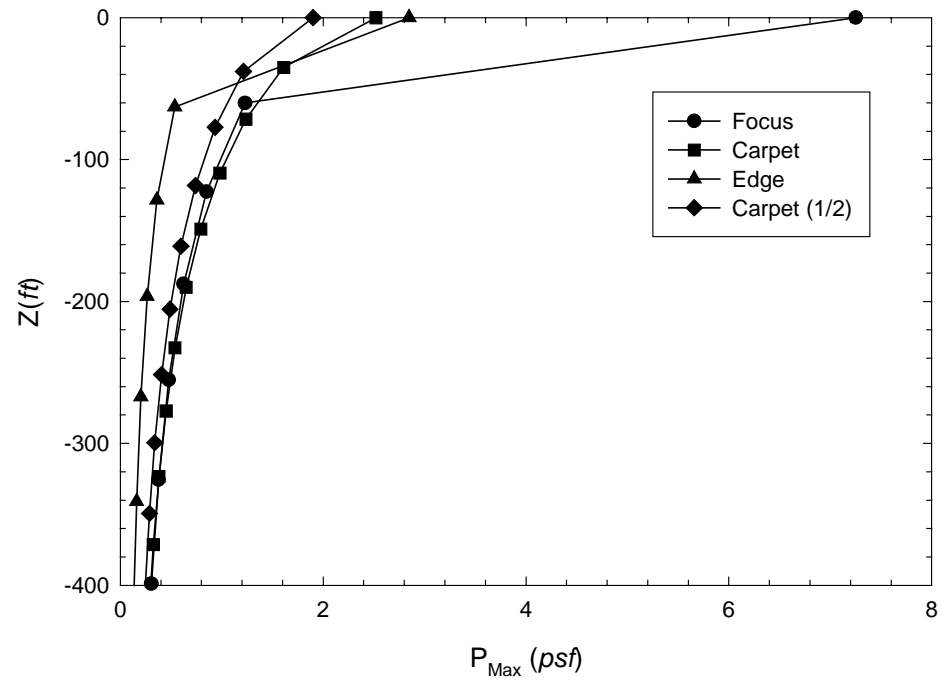


Figure O-7

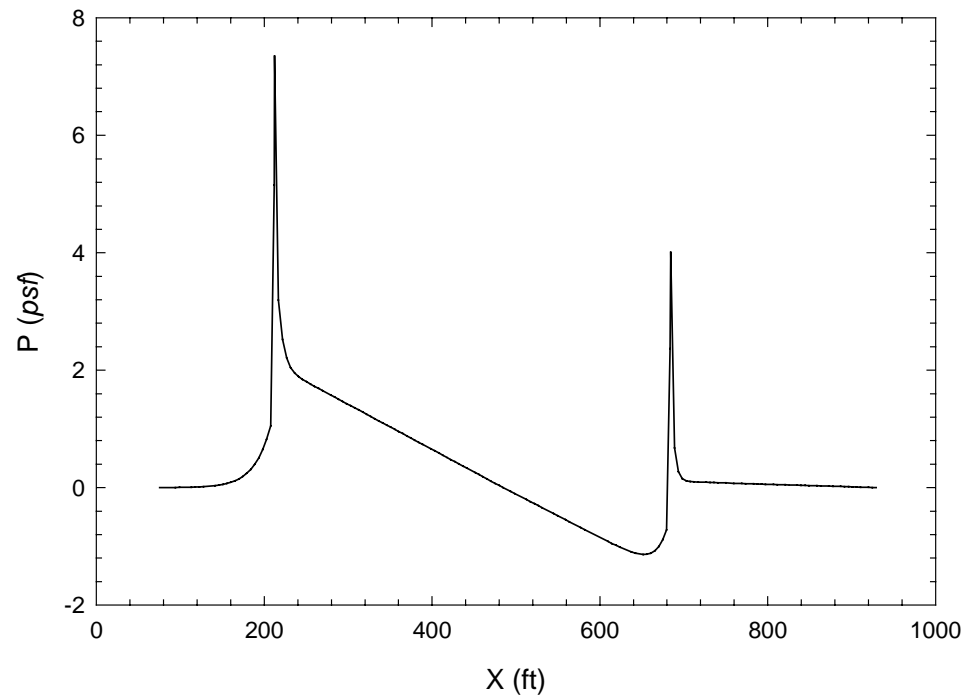


Figure O-8

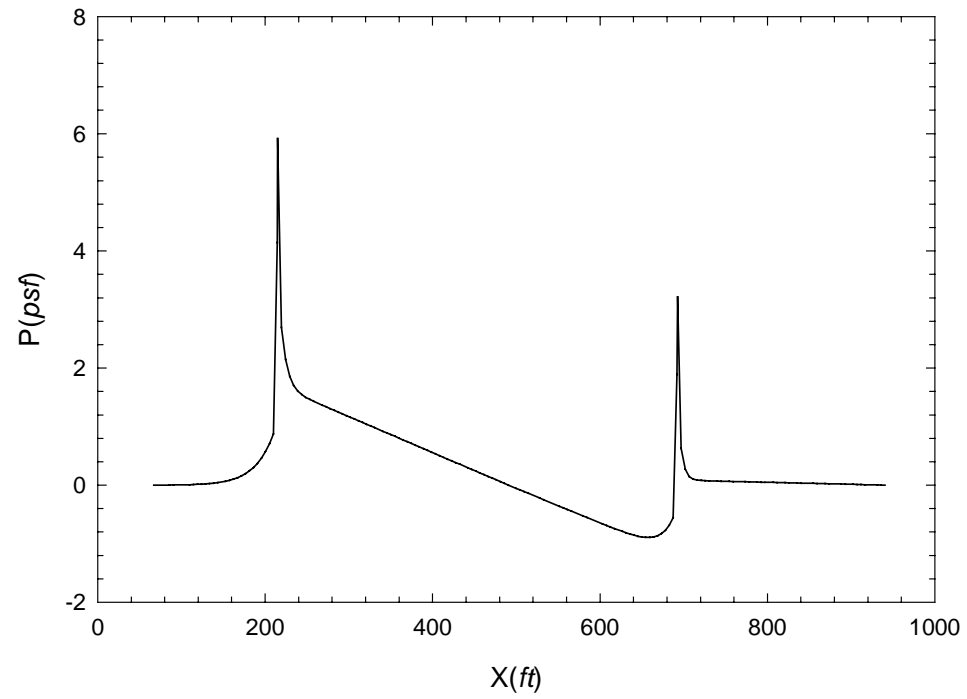


Figure O-9

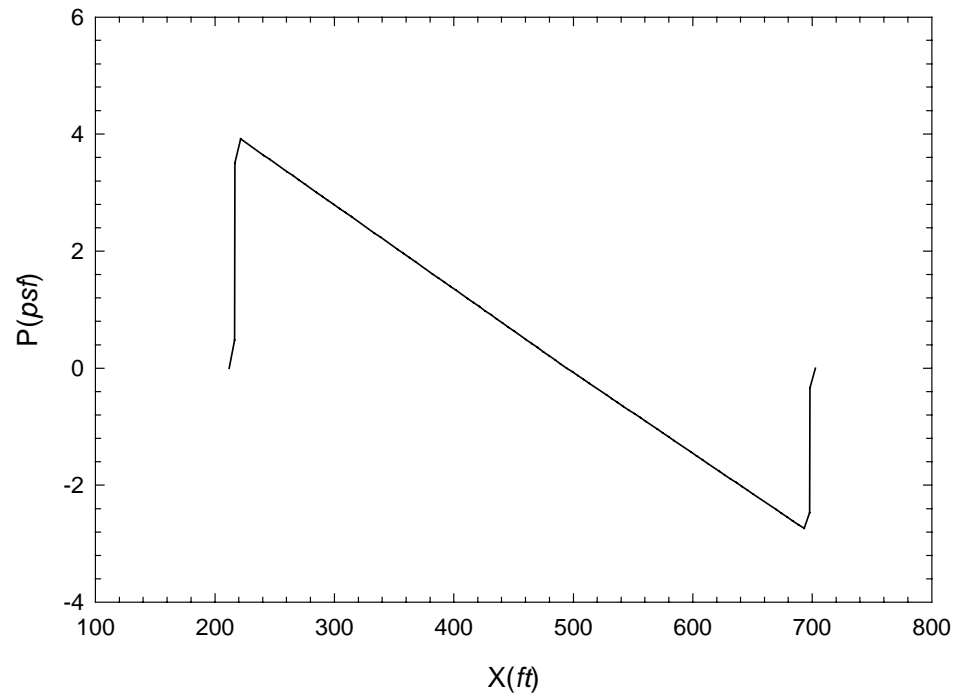


Figure O-10

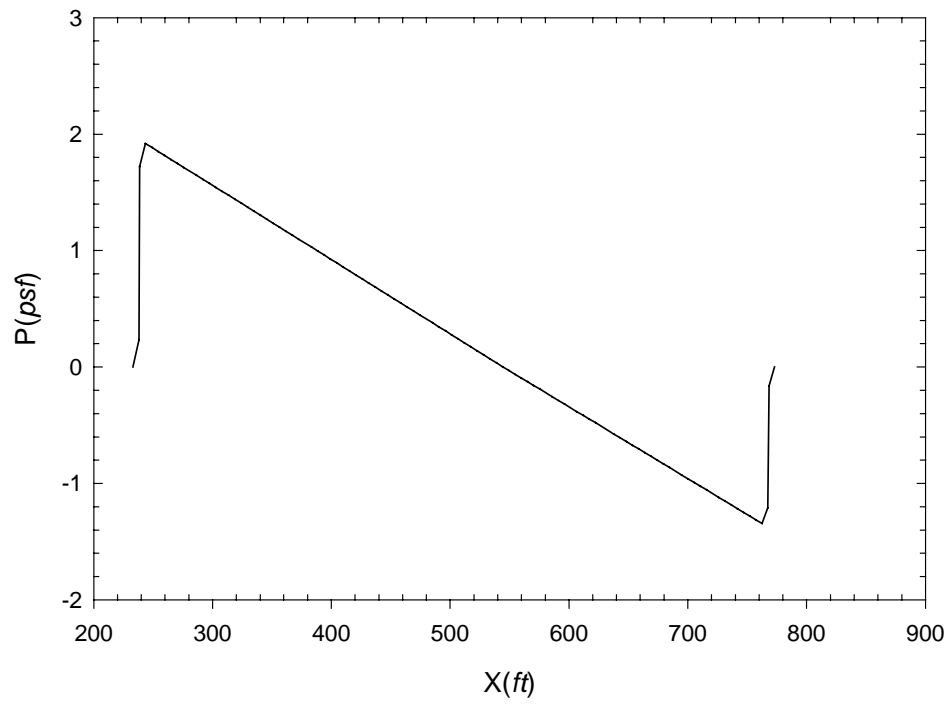


Figure O-11

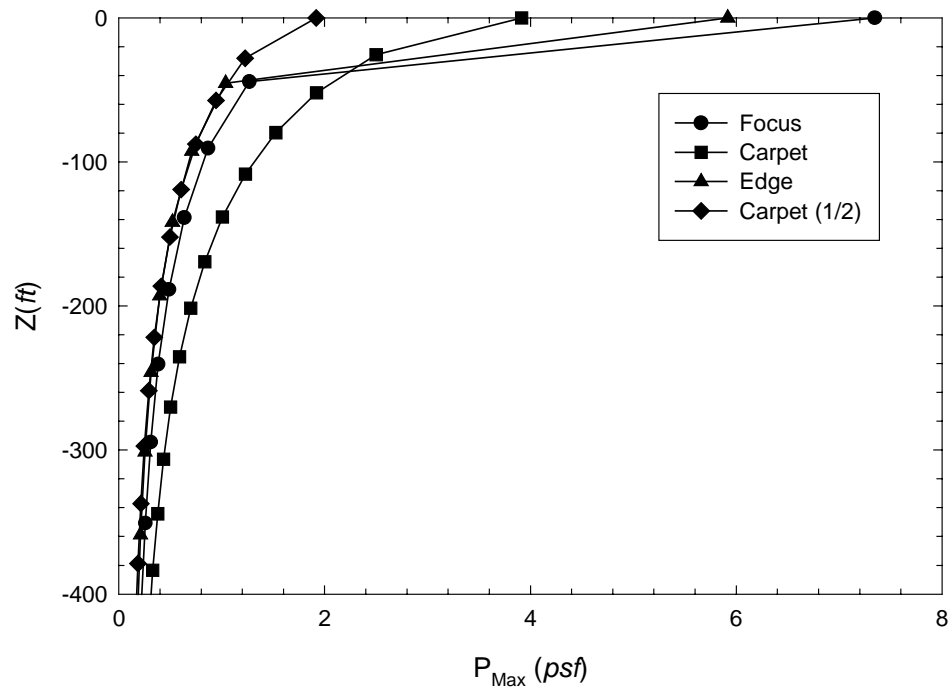


Figure O-12

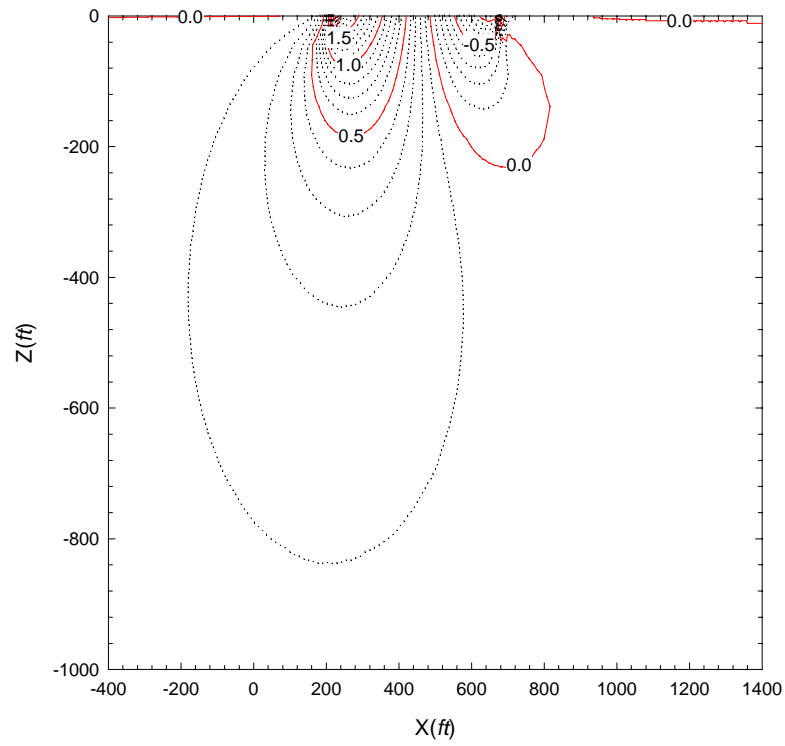


Figure O-13

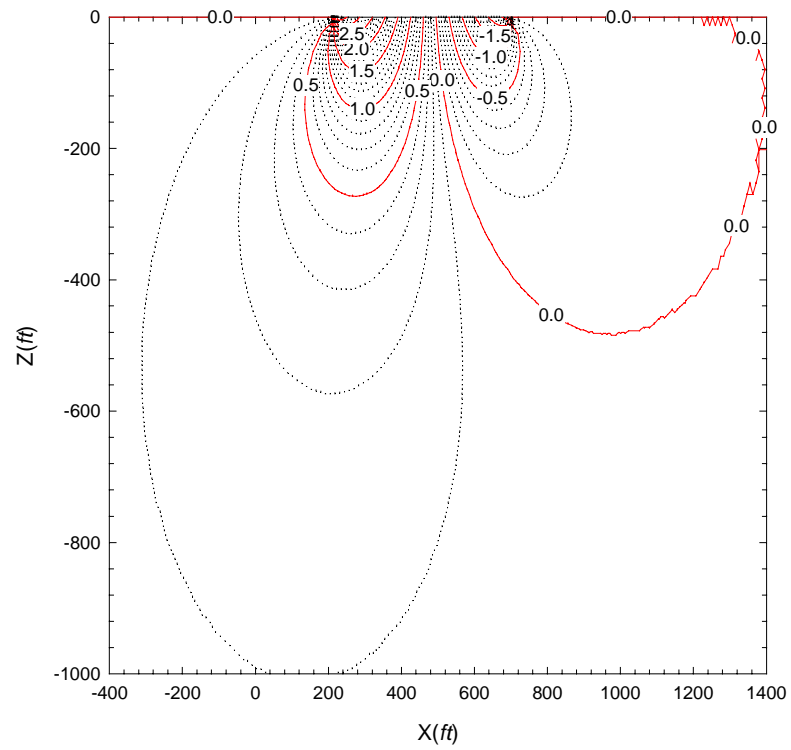


Figure O-14

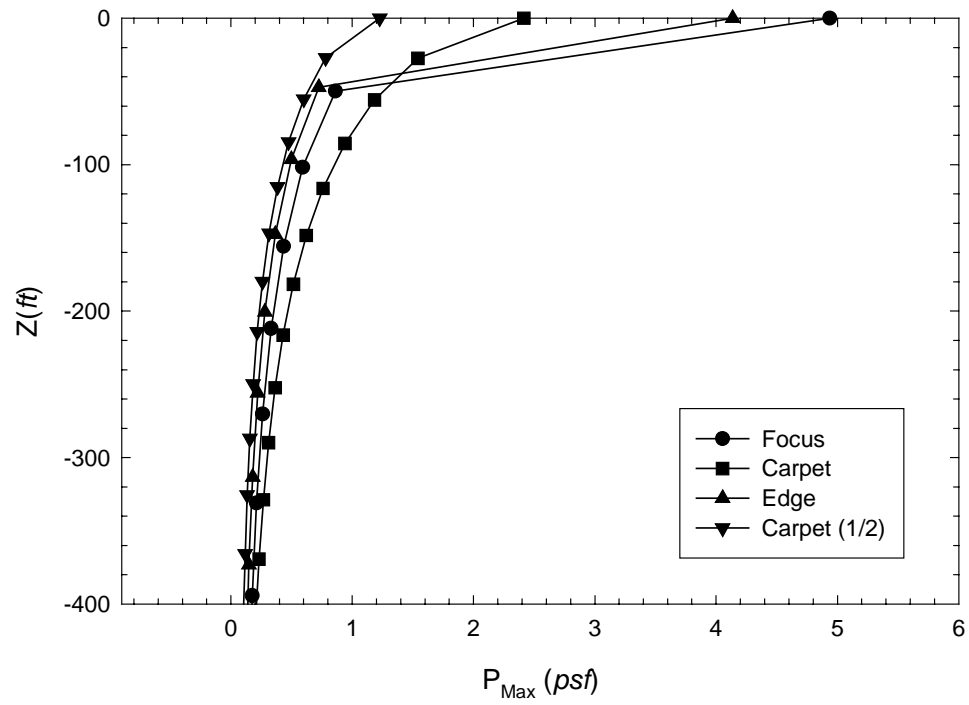


Figure O-15

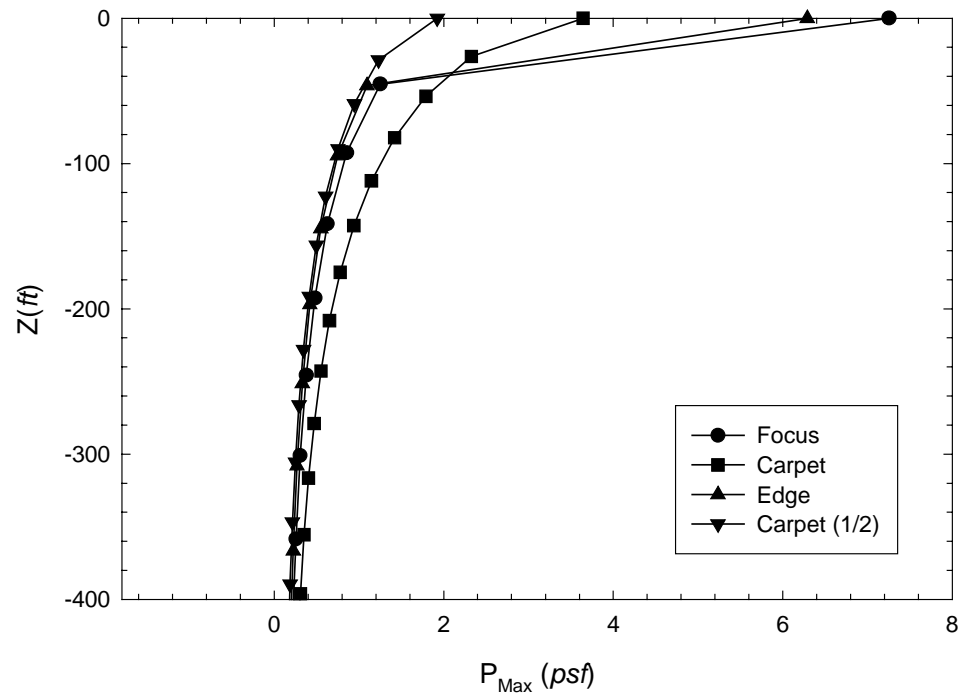


Figure O-16

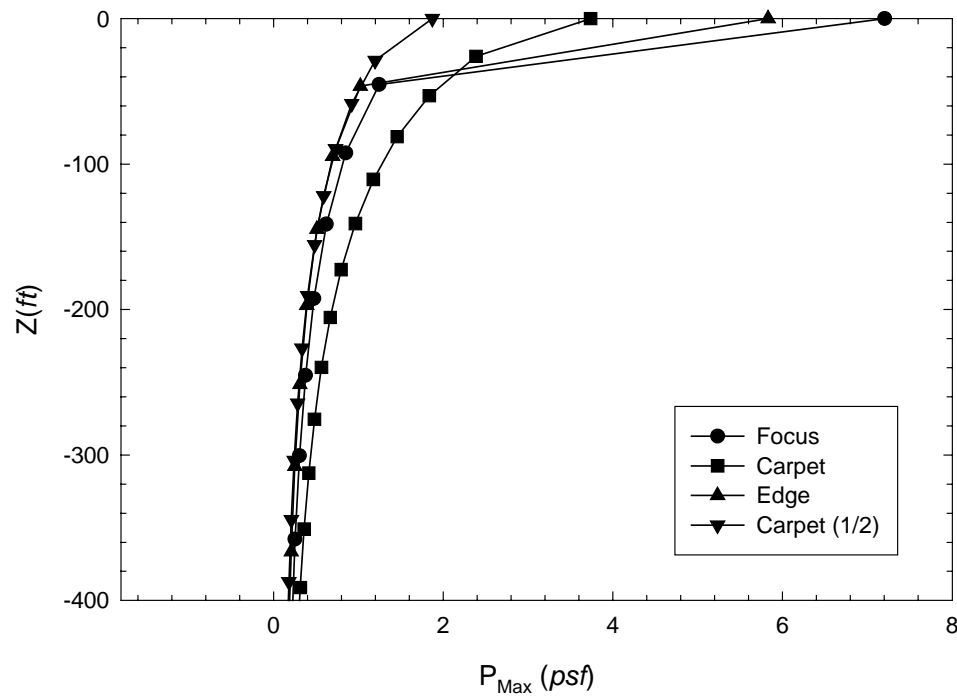


Figure O-17